INTERACTION OF COOLED ION BEAMS WITH INTERNAL FIBER TARGETS

B. v. Przewoski, H.O. Meyer, W. Lozowski, H. Nann, S.F. Pate,
R.E. Pollock, T. Rinckel, P. Schwandt, F. Sperisen, and W. deZarn
Indiana University Cyclotron Facility, Bloomington, In. 47408

H. Rohdjess and W. Scobel
Universitaet Hamburg, D-2000 Hamburg, Germany, Luruper Chaussee 149

Beam lifetime considerations and the limits of electron cooling restrict the thickness of internal targets to $\sim 10^{15}$ atoms/cm^2. Gas jets or diffuse gas targets are possible schemes, but require a major technical effort to maintain sufficient vacuum adjacent to the target region. In addition, some important target materials are not available as gases. Dust targets have been used successfully, but are comparable to gas targets in the required technical effort. Fiber targets are a relatively easy way to present certain target nuclei (such as ^{12}C, ^{28}Si, ^{54}Cu) to the stored beam. For fiber targets the idea is that the passage of a beam ion through a relatively thick object can be tolerated as long as the particle misses the fiber often enough. This allows sufficient cooling in many turns around the ring.

For simplicity we consider a vertical fiber of linear density ξ (atoms/cm) positioned at the center of the stored beam, whose horizontal width is $2a_o$. Then the average target thickness is[1]

$$d = \frac{2\xi}{\pi a_o}$$

A typical fiber, see below, has a linear density of ξ=10^{15} atoms/cm. If such a fiber is centered with respect to a 1 mm wide beam the resulting target thickness is 1.3×10^{16} atoms/cm^2. This thickness is too large, because it causes a beam lifetime short in comparison with the overhead time of a typical Cooler cycle, resulting in a low average luminosity. A lower average target thickness can be achieved by periodically moving the fiber across the entire profile of the beam. For sufficiently high velocities of the target motion ($\geq$ 5 cm/s) each beam particle has an equal chance to hit the target. For harmonic motion of the fiber with an amplitude x_o which is large compared to the width of the beam, the time-averaged target thickness becomes

$$d = \frac{\xi}{\pi x_o}$$

Moving the fiber across the beam introduces a time-dependent luminosity, whose time average can be adjusted by changing the amplitude of the fiber motion. For a gaussian current density distribution the maximum luminosity is given by

$$L_{max} = \sqrt{\frac{2}{\pi}} \frac{I\xi}{a_o}$$

where I is the circulating beam current and a_o is the horizontal semiaxis, if the beam spot is assumed to be elliptical. The duty factor $q = L_{avg}/L_{max}$ is given by the ratio of time-averaged to maximum luminosity with $L_{avg} = I \cdot d$.

We have developed a method to oscillate micro-ribbons with amplitudes between 2.5 and 10 mm, thus achieving target thicknesses between 10^{14} and 10^{15} atoms/cm^2. The setup is shown in Fig. 1. The ribbon target is mounted on a light-weight aluminum frame, which is attached to a support frame by four springs. Small permanent magnets are fixed on either side of the target frame. The transverse motion at a resonance frequency of 30 Hz is driven by applying an AC current to coils which are mounted on either side of the frame. Changing the current in the coils changes the amplitude of the target motion, and thus the target thickness. The support frame is mounted on a linear vacuum feedtrough in order to be able to move the oscillating target into the beam before data taking starts and retract it from the beam for injection.

So far, we have tested carbon ribbons with proton beams at 148 and 185 MeV. The manufacturing process of the ribbons has been developed at IUCF[2] and involves electron-beam evaporation of graphite through a mask onto a substrate. The mask consists of parallel, 50 μm tungsten wires, spaced by 15–60 μm. During evaporation the substrate rests on the wires. The deposited thickness is on the order of 8-10 μg/cm^2. As a substrate we use either glass or ferrotype steel. For glass, the lifting agent is a solution of betaine monohydrate, sucrose and water, while for steel we use soap (Tergitol 8, Union Carbide). The fibers are floated off the substrate in water, picked up and dried in a gentle air stream. We have examined fibers, which have been manufactured using both combinations of substrate and lifting agent, with an scanning electron microscope. Fig. 2 shows the surface structures of both types of fibers. Clearly the fibers which have been evaporated onto ferrotype steel have a smoother surface structure and therefore a more uniform thickness.

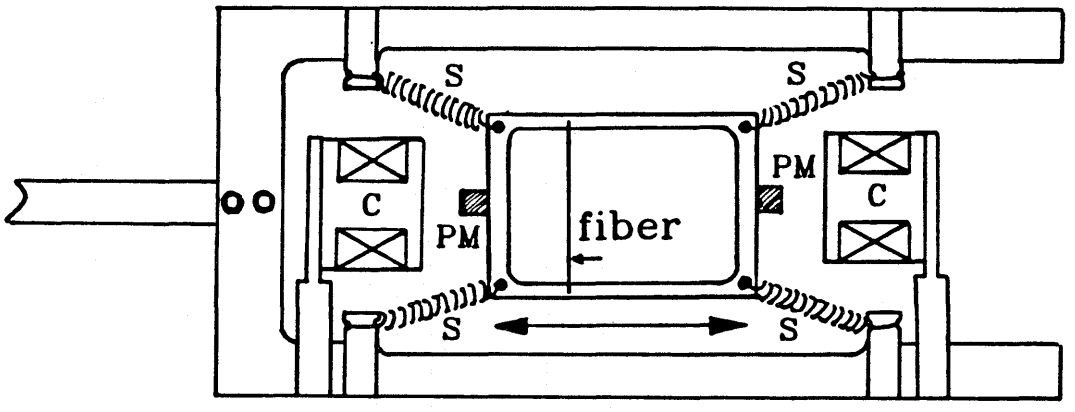

Figure 1. Device to oscillate a target fiber at variable amplitude. A 30 Hz mechanical resonance of a light frame suspended from springs (S) is excited via the permanent magnets (PM) in the alternating field of two coils (C).

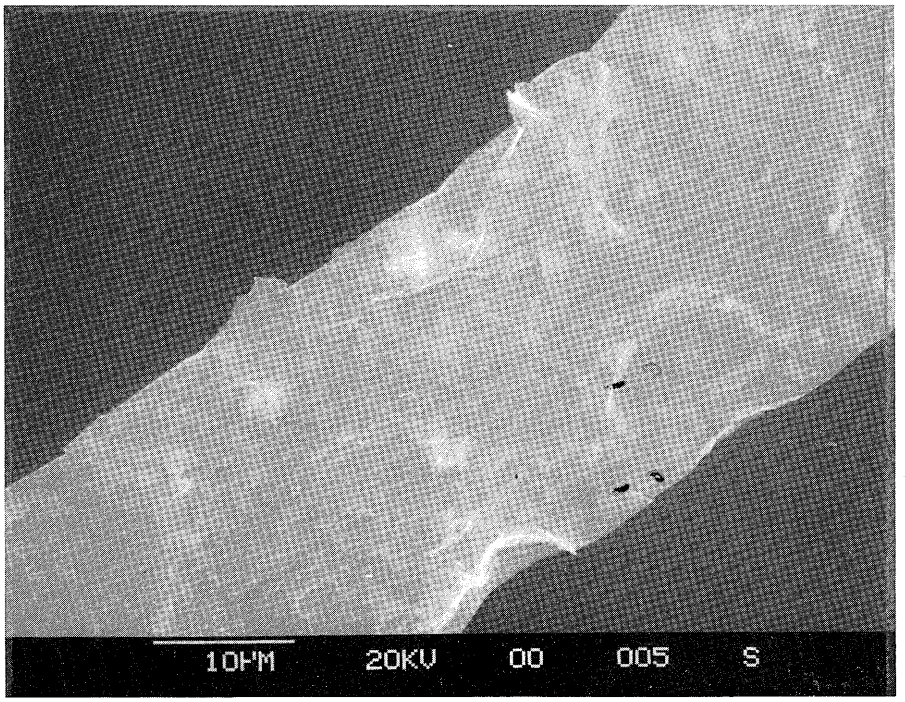

a)

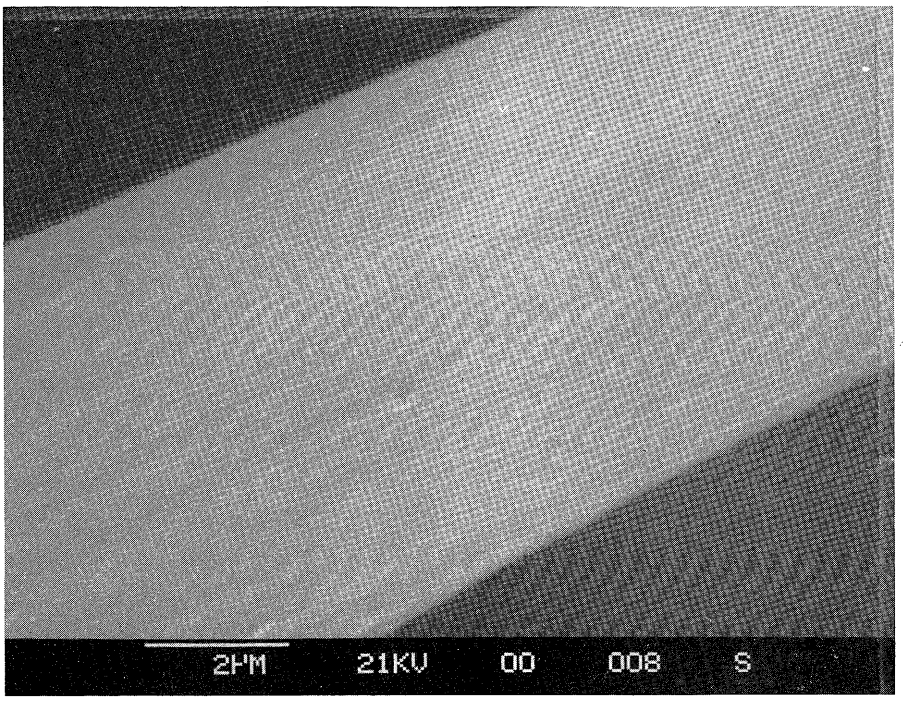

b)

Figure 2. Scanning electron microscope pictures from ^{12}C fibers. 2a shows a fiber evaporated onto a glass plate with betain as the parting agent. 2b shows a fiber evaporated onto ferrotype steel with tergitol as the parting agent.

The assumption of a time-averaged target thickness for fiber targets as compared to homegeneous targets has been investigated by means of a Monte Carlo simulation.[3] The interaction of the beam particles is treated by following the phase space coordinates of a sample of stored ions around the ring. Each particle is described by six independent variables, namely x_i, $\theta_{x,i}$, y_i, $\theta_{y,i}$, $p_i = (p_{s,i} - p_o)$ and ϕ_i. At the target location the beam is characterized by the radial aperture functions β_x, β_y and the dispersion η. The parameter set that describes the ring contains the betatron tune, the emittance and the x- and y-acceptances. The transverse motion of the fiber target is treated by calculating the time-dependent fiber position for a harmonic motion. The frequency and amplitude of the fiber motion are variable. Longitudinal and transverse heating are only taken into account if a particle hits the fiber. On each revolution the effects of longitudinal and transverse cooling are calculated. The transverse and longitudinal cooling force are calculated from measured parameters of the e^- cooling system. Effects that depend on beam brightness such as space charge effects and intra-beam scattering are neglected. The Monte Carlo program also contains the option to 'switch on' the RF-cavity, thus allowing the calculation to follow the motion of particles inside a bucket. After a completed revolution a particle is further processed only if it is still within both the geometrical and momentum acceptance of the ring.

Beam lifetimes and energy spreads have been calculated for a number of target thicknesses at 185 MeV for ^{12}C and N_2 (Figs. 4,5). The calculated lifetime and energy spread for the fiber and the homogeneous target are similar. Thus, the calculation indicates that the target thickness can indeed be time-averaged.

In a series of measurements we investigated the behavior of the beam with a ^{12}C-fiber target under varying conditions such as different beam energy (148 and 185 MeV) and different target location (η=0 and η=4 m). The target used was 8 $\mu g/cm^2$ thick and 43 μm wide. For comparison we took data with a homogeneous N_2 target under identical conditions. For both targets we measured the lifetime and the beam energy spread as a function of the target thickness. The beam energy spread was measured using a resonant Schottky pickup tuned to the 29^{th} harmonic of the revolution frequency.

Since the basic element in operating a fiber target is a single passage of the fiber across the beam, we took data on fractional beam loss per fiber passage and varied the speed at which the fiber was moved. Fig. 3 shows data taken at 148 MeV in a dispersed (G) section of the ring. The open and filled symbols indicate the direction of motion of the fiber, i.e. from inboard to outboard or vice versa. Due to the dispersion the beam loss is not the same in both directions. Comparison to a Monte Carlo calculation (solid line in Fig. 3) shows disagreement with respect to both the magnitude of loss per passage and the difference in loss between the two directions of motion. Placing the fiber in a non-dispersed (T) section under otherwise identical conditions yields essentially the same beam loss per fiber passage, the only difference being that the beam loss for the two directions of motion is equal.

Fig. 4 shows a comparison of measured lifetimes vs. the time-averaged target thickness for a carbon fiber (8$\mu g/cm^2$, 43 μm wide) that was oscillated at a frequency of 30 Hz and a homogeneous N_2-target at the same location in the ring (G-section, η=4 m). Monte

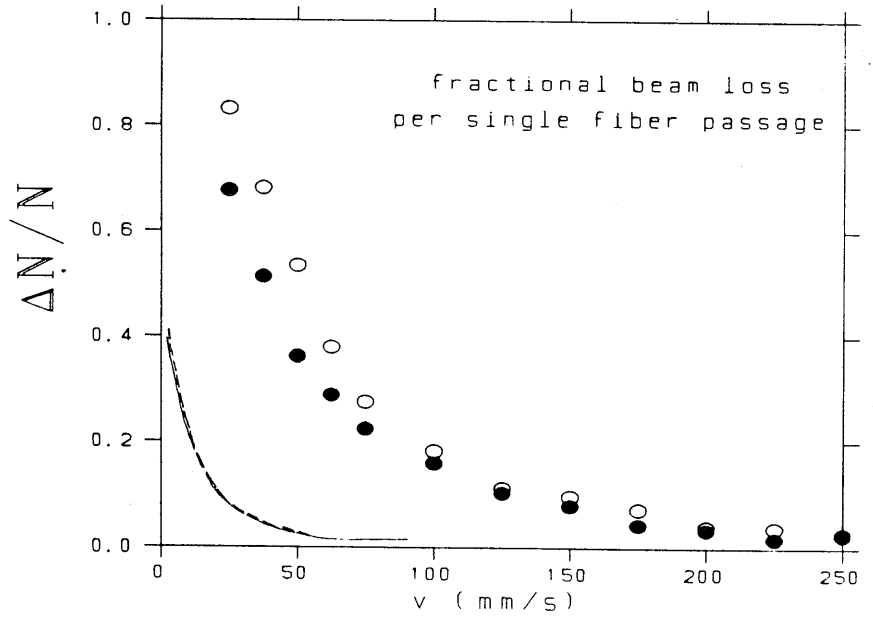

Figure 3. Fractional beam loss for a single fiber passage vs. velocity of the fiber. The fiber was positioned in a dispersed section of the ring. The open and filled symbols correspond to the fiber moving from inboard to outboard and vice versa. The lines represent Monte Carlo calculations for the two directions of motion. The incident beam energy was 148 MeV.

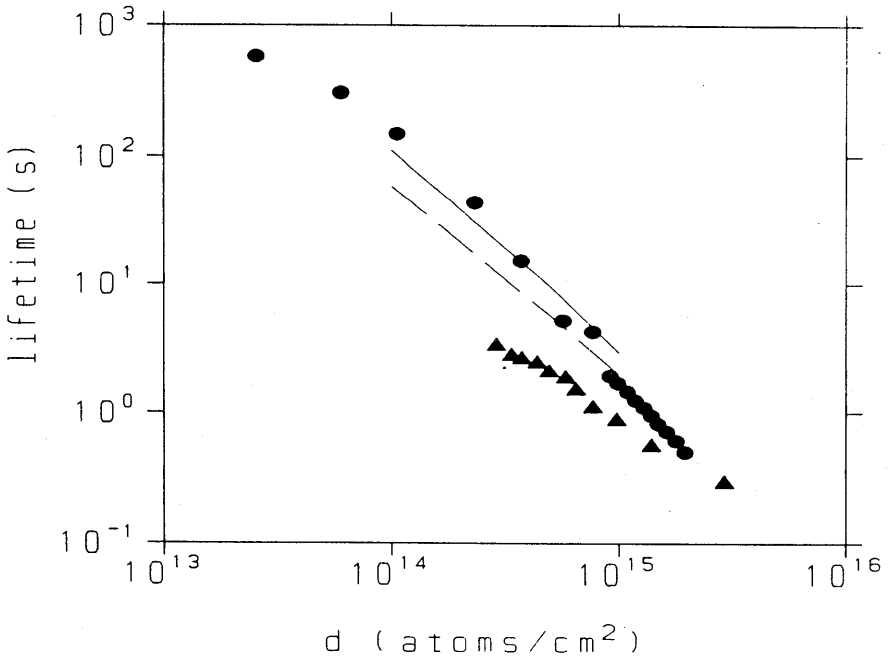

Figure 4. Lifetime τ of a 185 MeV proton beam for a carbon fiber target (triangles) and a homogeneous N_2 gas target (dots) vs. the target thickness. The solid and dashed lines represent Monte Carlo calculations for N_2 and carbon fiber targets respectively.

Carlo simulations for both cases are shown together with the data. In the case of the gas target the calculation agrees with the data whereas for the fiber target the measured lifetimes are lower than the calculation by an order of magnitude for the smaller target thicknesses ($\sim 10^{14}$). For larger target thicknesses ($\sim 10^{15}$) the agreement is somewhat better. Since the lifetime scales with Z^{-2}, the lifetime for ^{12}C is expected to be longer than for N_2. A measurement in a non-dispersed section of the ring under otherwise identical conditions gives the same disagreement between calculation and data for the fiber target. The possibility that the thickness of the fiber is not known well enough has been ruled out by calculating the target thickness from the measured yield, the cross section of p-^{12}C-scattering[4] and the beam current. The scattered protons were detected with the CE01-detector.[5] The deduced target thickness is consistent with the thickness measured during the evaporation.

In addition to the lifetimes, we measured Schottky signals for both the fiber and the gas target. Fig. 5 shows the comparison between carbon-fiber and N_2 gas, both having the same thickness, 4×10^{14} atoms/cm^2. The gas target affects the beam energy spread very

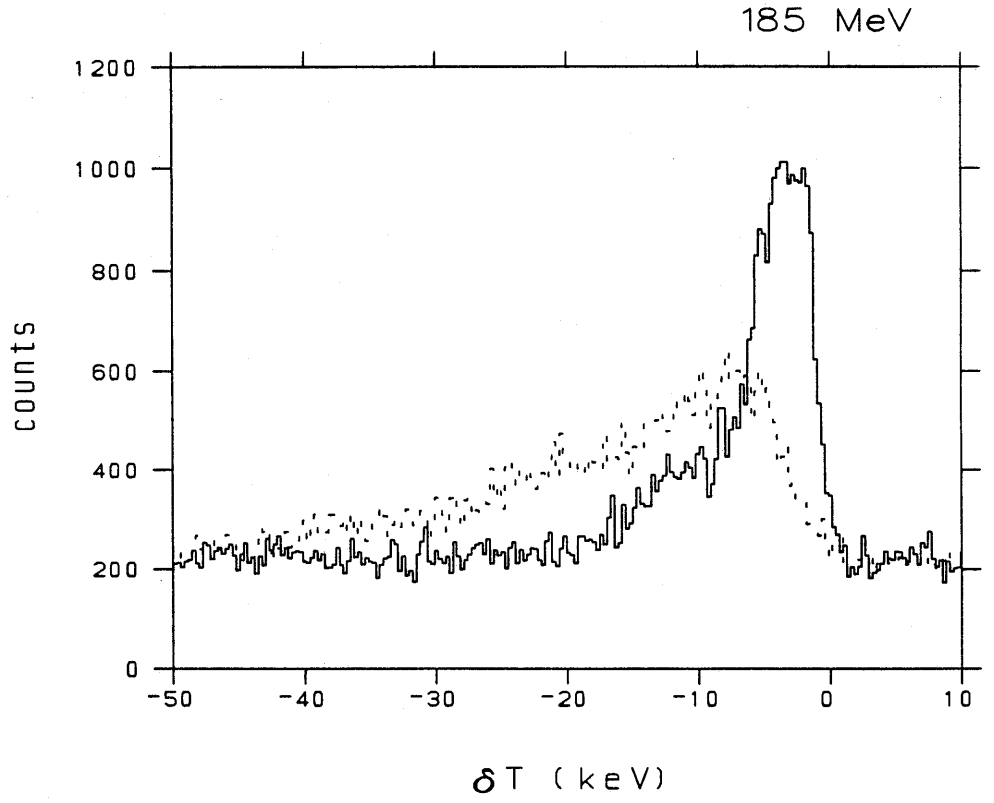

Figure 5. Schottky signals of a 185 MeV proton beam for a carbon fiber target (dashed) and a homogeneous N_2 gas target (solid). In both cases the target thickness was 4×10^{14} atoms/cm^2.

little (ΔT_{FWHM}=7 keV as compared to ΔT_{FWHM}=6 keV without target). This is true even for larger target thicknesses ($\Delta T_{FWHM} \leq 9$ keV for up to 10^{15} atoms/cm^2). In the case of the fiber target the energy spread not only increases rapidly with target thickness (ΔT_{FWHM}=14.8 keV for 4×10^{14} atoms/cm^2) but also develops a long tail towards the low momentum side of the peak. The Monte Carlo calculation fails to reproduce the difference in lifetime and energy spread between a fiber and a gas target.

In summary, we have measured the lifetime and beam energy spread for a carbon fiber and a homogeneous N_2 target as a function of target thickness in the range of $10^{14} - 10^{15}$ atoms/cm^2 under well defined operating conditions of the Cooler. The lifetime for the carbon fiber at d$\sim10^{14}$ atoms/cm^2 is shorter by an order of magnitude than for the homogeneous target of the same thickness. A Monte Carlo code that contains longitudinal and transverse target effects as well as longitudinal and transverse cooling and the RF-cavity fails to explain the short lifetime for the fiber target. The calculation is in good agreement with the data for the homogeneous target. Future work will be geared towards understanding and possibly eliminating the reason that causes the poor lifetime and beam energy spread for fiber-targets.

1. H.O. Meyer, Proc. Workshop on Nuclear Physics with Stored, Cooled Beams 1984, AIP Proc. No. 128, p. 76.
2. W.R. Lozowski and J.D. Hudson, Proc. 15th World Conf. of the INTDS (Santa Fe, Sept. 1990) Nucl. Instr. and Meth. A, to be published.
3. H.O. Meyer, Beam Properties in Storage Rings with Heating and Cooling, Nucl. Instrum. Meth. B10/11 (1985) 342.
4. H.O. Meyer, P.Schwandt, W.W. Jacobs, and J.R. Hall, Phys. Rev. **C27** (1983) 459.
5. H.O. Meyer, A. Ross, R.E. Pollock, A. Berdoz, F. Dohrmann, J.E. Goodwin, M.G. Minty, H. Nann, P.V. Pancella, S.F. Pate, B. v. Przewoski, T. Rinckel, and F. Sperisen, Total Cross Section for p+p$\rightarrow$p+p+π^0 near Threshold Measured with the Indiana Cooler, Phys. Rev. Lett. **65** (1990) 2846.